Proceedings of the 17th World Congress
The International Federation of Automatic Control
Seoul, Korea, July 6-11, 2008

Vibration Control of a Flexible Link Manipulator Using Smart Structures

H. Salmasi*. R. Fotouhi, P. N. Nikiforuk *****

*, **, *** *Mechanical Engineering Department, University of Saskatchewan, Saskatoon, Canada;*
email:hamid.salmasi@usask.ca, reza.fotouhi@usask.ca, peter.nikiforuk@usask.ca

Abstract: The active vibration suppression of a flexible link manipulator using a smart structure (piezoelectric actuator) is investigated. For this purpose, a Finite Element (FE) model is developed for the modal and transient analysis of a cantilever beam and a flexible link manipulator. The novelty of this work is in the development of an accurate finite element model of a piezoelectric and beam/manipulator. Also, the effect of the placement of the piezoelectric actuator along the beam, based on the controllability of the system states and using FE analysis, is investigated. To avoid system instability, a collocated sensor-actuator pair is used and a proportional control strategy is employed to adjust the voltage applied to the piezoelectric actuator so as to control vibrations. For the flexible link manipulator, it is shown that the vibration is well suppressed during and at the end of a maneuver by locating the piezoelectric actuator at the optimum location. The effect of the controller gain on the vibration behavior of the system is investigated and the optimum controller gain is found using two main evaluation criteria; these are the contribution of the dominant frequencies in the response and the error norms of the vibration amplitudes.

1. INTRODUCTION

Designing and utilizing robot manipulators having higher load capacities is always desired. However, vibration is an important factor that restricts the performance of such devices especially in applications where accurate positioning is very important. In the past decade different approaches have been used for vibration suppression. Active vibration control is one of the best approaches to suppress vibration. One of the methods of active control is using piezeoelectrics as actuators (Lewis and Inman, 2001).

Piezoelectric actuators have been successfully used for vibration suppression in some works. Khajehpour and Golnaraghi (1997) developed a nonlinear controller for vibration control of a cantilever beam using piezoelectric actuators. The optimum placement of the actuators for a cantilevered plate was proposed in (Peng et al., 2005). Effect of the placement of the piezoelectric actuator on the modal and spatial controllability of a structure was analysed in (Moheimani and Ryall, 1999) based on a performance index H_2. This index represents the norm of the input-output characteristics of a dynamical system and can be used to find the optimal placement of the actuator/sensor for plates.

However, in most of the models developed for the control of flexible structures, the controller is designed for a particular range of frequency, and it is common practice to remove the higher modes of vibration which are lying out of the desired range of frequency (Clark, 1997). This approach leads to truncation errors and the closed-loop performance will be considerably different from the predicted theoretical model. In fact, by ignoring the higher modes in the assumed mode shapes method, the zeros of the system are located far from where they should be and as a result the developed model will be different from the original one. One of the methods used to reduce the truncation error is finite element analysis (FEA) (Theodore and Ghosal, 1995). Since a large number of the mode shapes of the system are considered in FEA, the truncation of the error, due to ignoring the higher modes, is minimized in finite element models provided that a reasonably enough number of elements are used.

The main contribution of this paper is in the development of an accurate model of a piezoelectric and beam/manipulator using the finite element (FE) method and finding the optimal placement of the piezoelectric actuator along the flexible structure. Verifying the FE model by analytical calculations and error analysis can be considered as other less important contributions of this paper. It is believed that in the FE model, if the time integration and iterative solver provide accurate solutions, the computer simulations of the manoeuvre of the manipulators, even very flexible ones, will be quite reliable and closer to the experimental measurements. To check the accuracy of the FE model, the natural frequencies of the FE model are calculated and verified using the theoretical approach. The optimal placement of the piezoelectric is then found for the cantilevered beam, based on the controllability of the system, and is then compared with the results of the FEA. In the following, the piezoelectric is utilized for the vibration suppression of the flexible manipulator during the manoeuvre and after reaching the desired position. The effect of the gain on the controller performance is also investigated.

2. MATHEMATICAL FORMULATION

2.1 Piezoelectric Actuator

A cantilever beam with a piezoelectric actuator, shown in Fig. 1, was used in the study described in this paper. For perfectly bonded piezoelectric actuators and assuming an Euler-Bernoulli beam, the moment induced by the applied

voltage on the piezoelectric actuator is given as

$$M_p = E_p e_{31}[(V_1(t) - V_2(t))(t_b/2 + t_p/2)] \quad (1)$$

where E_p is the module of elasticity of the piezoelectric element, e_{31} the piezoelectric actuator constant, t_b the thickness of the beam and t_p the thickness of the piezoelectric actuator. $V_1(t)$ and $V_2(t)$ are respectively the applied voltage to the top and bottom surfaces of the piezoelectric actuator, and M_p is the effective bending moment applied to the beam with an equivalent area moment of inertia I_{eq}. By letting $K_s = (1/2)E_p e_{31}(t_b + t_p)$, equation (1) becomes

$$M_p = K_s(V_1(t) - V_2(t)) \quad (2)$$

If the applied voltage to the bottom surface of the piezoelectric actuator is zero ($V_2(t) = 0$), then from equation (2) M_p will be proportional to the applied voltage on the top surface, $M_p = K_s V_1(t)$. If the beam is modeled as a Euler-Bernoulli beam with deflection $y(x,t)$, where x is measured from the fixed end of the beam and t is time, the partial differential equation of the system becomes

$$E_b I_{eq}\frac{\partial^4 y(x,t)}{\partial x^4} + \rho_b A_b \frac{\partial^2 y(x,t)}{\partial t^2} = M_p \frac{\partial}{\partial x}[\delta(x - L_s - L_p) - \delta(x - L_s)] \quad (3)$$

where E_b and ρ_b are the module of elasticity and density of the beam respectively. L_b, L_p and L_s, as shown in Fig. 1, are the length of the beam, length of the piezoelectric actuator, and distance of the piezoelectric actuator from the fixed end respectively, and $\delta(x)$ is the Dirac function. The deflection of the beam can be expressed using assumed mode shapes

$$y(x,t) = \sum_{i=1}^{N} \varphi_i(x) q_i(t), \qquad i = 1,2,\cdots,N \quad (4)$$

where φ_i is the i'th normalized mode shape, q_i is the amplitude of the i'th normalized mode shape, and N is the number of the assumed mode shapes. Substituting equation (4) into equation (3), multiplying by φ_i and integrating, equation (3) becomes

$$E_b I_{eq} q_i(t)\int_0^{L_b} \frac{\partial^4 \varphi_i(x)}{\partial x^4}\cdot\varphi_j(x)\,dx + \rho_b A_b \ddot{q}_i(t)\int_0^{L_b}\varphi_i(x)\varphi_j(x)\,dx = K_s V_1[\varphi_i'(x - L_s - L_p) - \varphi_i'(x - L_s)], i, j = 1,2,\cdots,N \quad (5)$$

where the dot indicates the time derivative and $(\,)'$ represents the derivation with respect to x. Using the orthogonality property of mode shapes and inclusion the modal damping ratio ξ_i for the i'th normal mode, equation (5) is written as

$$\ddot{q}_i(t) + 2\xi_i\omega_i\dot{q}_i(t) + \omega_i^2 q_i(t) = F_i V_1(t), \quad i = 1,2,\cdots,N \quad (6)$$

where

$$\omega_i^2 = \frac{E_b I_{eq}}{\rho_b A_b}\int_0^{L_b}\frac{\partial^4\varphi_i(x)}{\partial x^4}(x)\varphi_i(x)\,dx, \quad i = 1,2,\cdots,N \quad (7)$$

$$F_i = \frac{K_s}{\rho_b A_b}[\varphi_i'(x - L_s - L_p) - \varphi_i'(x - L_s)], \quad i = 1,2,\cdots,N \quad (8)$$

Equation (6) can be written in the state-space form

$$\dot{X}(t) = AX(t) + FV_1(t) \quad (9)$$

where

$$X(t) = \begin{bmatrix} q_1(t) \\ \vdots \\ q_N(t) \\ \dot{q}_1(t) \\ \vdots \\ \dot{q}_N(t) \end{bmatrix}, \quad A = \begin{bmatrix} O_{N\times N} & I_N \\ -\Omega^2 & -2\xi\Omega \end{bmatrix}, \quad F = \begin{bmatrix} O_{N\times 1} \\ F_1 \\ \vdots \\ F_N \end{bmatrix} \quad (10)$$

and $\Omega = diag(\omega_1, \omega_2, \cdots, \omega_N)$, $\xi = diag(\xi_1, \xi_2, \cdots, \xi_N)$, $O_{N\times N}$ is a zero matrix of size N, and I_N is an identity matrix of size $N \times N$. Note that as shown in equation (8) the matrix F depends on the location of the piezoelectric, L_s.

The optimum placement of the piezoelectric can be obtained by minimizing the energy of the control force. In fact, it is desired in minimizing the energy required to steer the initial state $X(t_0)$ to the final state $X(t_1)$. It means that at the final state all modes are well suppressed; that is $q_i(t_1) = 0$ and $\dot{q}_i(t_1) = 0$ for $i = 1,2,\cdots,N$. Therefore the final state , $X(t_1)$, must be zero. The value of the minimum energy functional J of the control voltage $V_1(t)$, which steers the initial state $X(t_0)$ to zero, can be written as (Klamka, 1991)

$$J(t_0, t_1; X(t_0)) = X(t_0)^T W^{-1} X(t_0) \quad (11)$$

where W is a controllability Grammian matrix which is the solution of the following Lyapunov equation

$$WA^T + AW + FF^T = 0 \quad (12)$$

The controllability measure μ can be introduced as the reciprocal of the maximum value of the control energy $J(t_0, t_1; X(t_0))$ for all initial states taken from the unit sphere, that is, $\{X(t_0) \in R^n : \|X(t_0)\| = 1\}$; thus

$$1/\mu = \max_{\|X(t_0)\|=1} J(t_0, t_1; X(t_0)) = \lambda_{\max}(W^{-1}(t_0, t_1)) = 1/\lambda_{\min}(W(t_0, t_1))) \quad (13)$$

where $\lambda_{\max}(W^{-1}(t_0, t_1))$ denotes the maximum eigenvalue of W^{-1} which is the inverse of the minimum eigenvalue of W, $\lambda_{\min}(W(t_0, t_1))$. To find the optimal placement of the piezoelectric actuator, the control energy in equation (13), must be minimized for different locations of the piezoelectric actuator. In other words, most controllability can be obtained when μ has its maximum value. Based on this approach, the optimal placement of a piezoelectric actuator will be found in Section 4.1 for a cantilevered beam.

2.2 Dynamics of Manipulator

The manipulator shown in Fig. 2 has a hub at the base with a mass moment of inertia J_o, a beam of length L_b, a payload with mass m_p and a mass moment of inertia J_p. The coordinate system (X,Y) is the global coordinate system and (x,y) rotates with angular velocity $\dot{\theta}$ where the angle θ is the rotation of the base. A torque u is applied by the hub (motor) and the arm rotates around its base during the interval time of $(0 < t \le t_d)$. After reaching the desired angle θ_d, the torque is reduced to zero and the arm behaves as a cantilever beam $(t > t_d)$. Thus, the simulation procedure must be performed in two steps for a rotating flexible manipulator $(0 < t \le t_d)$ and a cantilever beam $(t > t_d)$. A piezoelectric actuator is used for vibration suppression of the manipulator during the rotation of the arm and after reaching its desired position.

2.3 Controller Design

A proportional controller was used in which the applied voltage to the piezoelectric actuator was proportional to the axial strain. A block diagram of the controller is shown in the Fig. 3 where K_c, ε, V and V_ε are the gain, strain at the midpoint of the piezoelectric actuator, potentiometer output voltage and applied voltage to the piezoelectric actuator, respectively. To avoid instability due to the non-collocation of sensor and actuators, the actuator and sensor were located at the same location; that is the strain ε was measured at the location of the piezoelectric actuator. The set point (for error) was selected as zero. An important issue in vibration control of flexible structures is the collocation of sensor and actuator. In this study, a collocated sensor-actuator pair is used. The collocation of sensor and actuator guarantees that the system is positive real at least for lower frequency modes. However, this guarantee does not apply to higher frequency modes, because the collocation principle does not apply to modes of wavelength comparable to the size of piezoelectric actuator. In addition, computational delays at high frequencies can drive some higher frequency modes unstable (Falangas, 1994). Therefore, the collocation of the sensor and actuator necessarily does not lead to the stability of the controller. Another factor affecting the stability criteria is the proper location of the piezoelectric which is discussed later in this paper.

3. FINITE ELEMENT MODEL

Three types of elements from the ANSYS Software elements library were used to model the beam/manipulator. The beam was constructed using ten "PLANE 82" elements spaced equally along the beam. This element had eight nodes with two degrees-of-freedom (DOF), and translations in the x and y directions at each node. Since "PLANE 82" did not have a rotational degree of freedom, two "BEAM 3" elements having three degrees of freedom, translations in the nodal x and y directions as well as rotation in the z-direction, were used for the base rotation. The element "PLANE 223", which models the piezoelectric actuator, was used as an actuator to suppress the vibration. The physical properties of the beam and piezoelectric actuator shown in Figs. 1 and 2, are given as follows

$L_s = 0.030\,m, L_b = 0.200\,m, t_b = 0.001\,m, I_b = 8.33\times10^{-11}\,m^4,$
$t_p = 0.001\,m,\ \nu = 0.300, \rho_b = 7.80\times10^3\,kg\cdot m^{-3}, J_o = 0\,kg.m^2,$
$J_p = 0\,kg.m^2, m_p = 0\,kg, E_b = 201\times10^9\,N.m^{-2}, L_p = 0.010\,m$

where L_b, L_p and L_s are, respectively, the length of the beam, length of the piezoelectric actuator, and distance of the piezoelectric actuator from the fixed end, and t_b and t_p are respectively the thicknesses of the beam and piezoelectric actuator. E_b, I_b, ν and ρ_b are the module of elasticity, area moment of inertia, Poisson ratio and density of the beam respectively, and m_p, J_o and J_p are the payload mass, mass moment of inertia of the hub and mass moment of inertia of the payload.

4. SIMULATION RESULTS

In the simulation study both modal and transient analyses were carried out for the cantilever beam and for the robot flexible link manipulator. The simulation was performed in three steps. In the first step, the free vibration and modal analysis of the cantilever beam was studied. The natural frequencies of the manipulator which were determined theoretically and using finite element analysis (FEA) are illustrated in table 1. The results obtained from the theoretical approach and FEA are in good agreement. In the next step, the effect of placement of the piezoelectric actuator on the vibration was studied and the optimal location of the piezoelectric actuator along the beam was determined. Finally, the active vibration suppression of the robot flexible link manipulator during and at the end the manoeuvre was successfully accomplished, and the effect of the gain on the vibration behaviour of the system was determined. In this study it was assumed that the base was fixed and the beam behaved as a cantilever.

4.1 Optimum location of the Piezoelectric Actuator

Based on the approach described in Section 2.1, the optimum placement of the piezoelectric was found for the cantilevered beam. For this purpose, the first two mode shapes were considered and the eigenvalues of the controllability Grammian matrix, W, were found for different locations of the piezoelectric actuator using the Lyapunov equation (12). Values of μ versus L_s / L_b, are plotted in Fig. 4. It can be seen that the location $L_s / L_b = 0.3$ had the maximum value and provided the most controllability.

To verify the optimal placement of the piezoelectric actuator, $L_s / L_b = 0.30$, the simulation was performed using the finite element model for different values of L_s / L_b. To find the best location of the actuator, the following evaluation criteria were used

$$E_{0-3} = \sqrt{\frac{1}{N_3 - 1}\sum_{i=0}^{i=N_3}\left(\frac{y_{i,e}}{y_{\max,e}}\right)^2} \quad (14)$$

$$E_{2-3} = \sqrt{\frac{1}{N_3 - N_2}\sum_{i=N_2}^{i=N_3}\left(\frac{y_{i,e}}{y_{\max,e}}\right)^2} \quad (15)$$

where the norms E_{0-3} and E_{2-3} represent the values of the normalized tip deflections for the time intervals of ($0 \le t \le 3$) and ($2 \le t \le 3$), respectively. The $y_{i,e}$ is the tip deflection of the beam at the time step i, N_3 is the number of time steps at $t = 3$ and N_2 is the number of time steps at $t = 2$. Table 2 illustrates the values of these norms for the different cases investigated. The values of E_{0-3} and E_{2-3} are plotted versus L_s / L_b in Fig. 5. According to this figure, $L_s / L_b = 0.3$ corresponds to the best location of the piezoelectric actuator. This finding is also consistent with the findings of (Peng, 2005) for a similar beam.

4.2 Flexible link robot manipulator

To verify the effectiveness of the piezoelectric actuator in suppressing the vibration of a robot manipulator, a single flexible manipulator was analyzed. In this case, the manipulator could rotate about its base. The physical properties and the dimensions were the same as those of the cantilever beam, except the values of the mass moment of inertia of the hub and the tip-mass which were selected as $J_o = 1.2e-3\, kg \cdot m$ and $m_p = 0.2\, kg$ respectively. The torque applied to the hub was of a bang-bang nature causing, as shown in Fig. 6.a, the manipulator initially to accelerate, then decelerate and finally to lock at its desired final position, where it continued to vibrate as a cantilever beam. As shown in Fig. 6.b, the hub rotated approximately 0.8 *rad* in one second and it was locked then at 0.8 *rad*. The natural frequencies of the manipulator and cantilever beam were obtained theoretically and compared in table 1 against the FEA results. Fig. 7.a illustrates the tip deflection with respect to the shadow beam (see Fig. 2) without the controller being active ($K_c = 0$). To find the dominant frequencies of the system, the FFT of the tip deflections in time was evaluated. This is illustrated in Fig. 7.b which indicates three dominant frequencies. The first was the main excitation frequency which was 1.0 *Hz* . The second frequency was approximately 17 *Hz* which corresponded to the first natural frequency of the cantilever beam and the third frequency, which was approximately 60 *Hz* , corresponded to the first non-zero natural frequency of the flexible link manipulator. To suppress the vibration a piezoelectric actuator was placed at the optimum location, $L_s / L_b = 0.3$, as reported in Section 4.1. The simulation was carried out for three different values of the controller gain, $K_c = 2.00e5, 4.00e5$ and $6.00e5$, and these are referred to as Cases 2, 3 and 4 respectively. The vibration was well suppressed during and at the end of the manoeuvre as shown in Fig. 8.a for Case 3 ($K_c = 4.00e5$). The FFT of the tip deflection in time is shown in Fig. 8.b for this case. According to this figure, the peak values of the dominant frequencies, especially the main excitation frequency and the first natural frequency of the cantilever beam, were significantly reduced for Case 3 in comparison with Case 1 (Fig. 7).

Three evaluation criteria, E_{0-1} for $0 \le t < 1$ (during the manoeuvre), E_{1-4} for $1 \le t < 4$ (at the end of the manoeuvre) and E_{0-4} for $0 \le t < 4$ (the total response), were defined so as to compare the results. The values of these norms were the normalized tip deflections of the manipulator arm and were calculated using equations similar to those reported for the cantilever beam (equations (14) and (15)). These norms are compared in Fig. 9.a for different gain values. As shown in Fig. 9.a, the gain value of Case 3 ($K_c = 4.00e5$) had the smallest values of norms E_{1-4} and E_{0-4} in comparison with other gain values. Thus the amplitude of vibration was smaller for Case 3 than other cases, after the manipulator reached its desired rotation during $1 \le t < 4$, as well as during the total response ($0 \le t < 4$).

Another index which was used to compare the results was the values of the PSD peaks at the dominant frequencies. This index is shown in Fig. 9.b for four different cases. Also, for the three dominant frequencies, overall Case 3 shows the best result in suppressing the vibration.

5. CONCLUSIONS

Finite element analysis (FEA) was used in this paper for modeling a cantilever beam and a flexible robot manipulator. The optimum values for the controller gain were found and the optimum location of the piezoelectric actuator was determined for the cantilever beam based on minimizing the energy of the control force and was verified by FEA. The controller was stable because of using a collocated sensor-actuator pair in the optimum position and because of using full non-linear transient dynamic analysis using FEA. Also, it was concluded that Case 3 with a controller gain of Kc= 4.00e5 and the location of the piezoelectric actuator 30% of the beam length from the base, produced the best results as far as suppressing the vibration was concerned. These findings were verified by analytical calculations and will be verified experimentally in near future.

REFERENCES

ANSYS Software ANSYS Inc., Canonsburg, PA, USA (www.ansys.com)

Chen C. Q. and Shen Y. (1997). "Optimal control of active structures with piezoelectric modal sensors and actuators," *Smart Materials and Structures* **6(4)** 403-9.

Clark R. L. (1997). "Accounting for out-of-bandwidth modes in the assumed modes approach: implications on collocated output feedback control," *Journal of Dynamic Systems, Measurement, and Control* **119(3)** 390-395.

De Luca A. and Siciliano B. (1991). "Closed-form dynamic model of planar multilink lightweight robots," *IEEE Transactions on Systems, Man and Cybernetics* **21(4)** 826-39.

Devasia S., Meressi T., Paden B. and Bayo E. (1993). "Piezoelectric actuator design for vibration suppression: placement and sizing," *Journal of Guidance, Control, and Dynamics* **16(5)** 859-64.

Falangas E. T., Dworak J. A. and Koshigoe S. (1994). "Controlling plate vibrations using piezoelectric actuators," *IEEE Control Systems Magazine* **14(4)** 34-41.

Khajepour A. and Golnaraghi M.F., (1997). "Experimental control of flexible structures using nonlinear modal coupling: forced and free vibration," *Journal of Intelligent Material Systems and Structures* **8(8)** 697-710.

Khorrami F., Zeinoun I. and Tome E. (1993). "Experimental results on active control of flexible-link manipulators with embedded piezoceramics," *Proc. of IEEE International Conference on Robotics and Automation* (Atlanta, GA, USA) **3** 222-227.

Klamka J. (1991). "*Controllability of dynamical systems*," Boston, Kluwer Academic Publishers.

Lewis J. A. and Inman D. J. (2001). "Finite element modeling and active control of an inflated torus using piezoelectric devices," *Journal of Intelligent Material Systems and Structures* **12(12)** 819-33.

Manning W. J., Plummer A. R. and Levesley M. C. (2000). "Vibration control of a flexible beam with integrated actuators and sensors," *Smart Materials and Structures* **9(6)** 932-39.

Moheimani S. O. R. and Ryall T. (1999). "Considerations on placement of piezoceramic actuators that are used in structural vibration control," *Proc. of the 38th IEEE Conference on Decision and Control* (Phoenix, AZ, USA) **2** 1118-23.

Peng F., Ng A. and Hu Y. (2005). "Actuator placement optimization and adaptive vibration control of plate smart structures," *Journal of Intelligent Material Systems and Structures* **16(3)** 263-71.

Theodore R. J. and Ghosal A. (1995). "Comparison of the assumed modes and finite element models for flexible multilink manipulators," *International Journal of Robotics Research* **14(2)** 91-111.

Table 1. The natural frequencies of the flexible manipulator and cantilever beam

	Flexible link manipulator		Cantilever beam	
Set	Theoretical (Hz)	FEA (Hz)	Theoretical (Hz)	FEA (Hz)
1	0	0	16.97	16.91
2	61.94	61.41	112.6	110.5
3	145.6	144.5	325.7	322.9

Table 2. Evaluation criteria for different locations of actuator

L_s / L_b	0.05	0.1	0.2	**0.3**	0.4	0.5
E_{0-3}	0.3917	0.2999	0.2848	**0.2845**	0.2938	0.3106
E_{2-3}	0.2084	0.0799	0.063	**0.063**	0.0731	0.0925

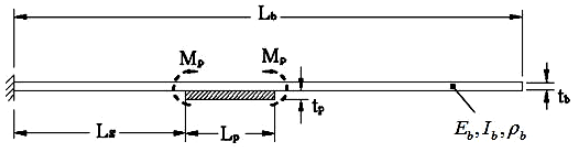

Fig. 1. Model of a cantilever beam with piezoelectric actuator

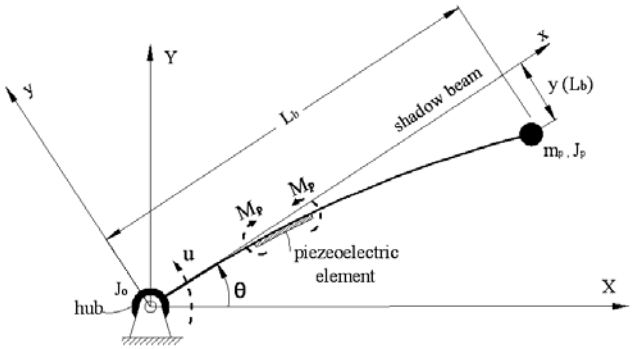

Fig. 2. A single flexible link robot manipulator including its tip mass and hub inertia

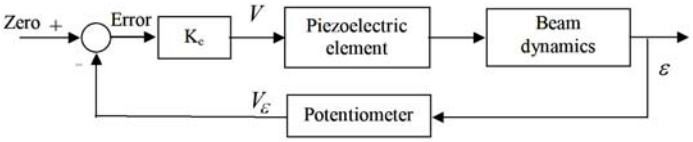

Fig. 3. Block diagram of the controlling vibration of the manipulator

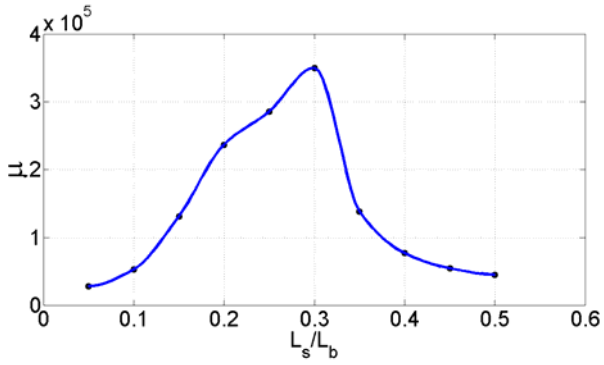

Fig. 4. Controllability measure for different locations of the piezoelectric actuator

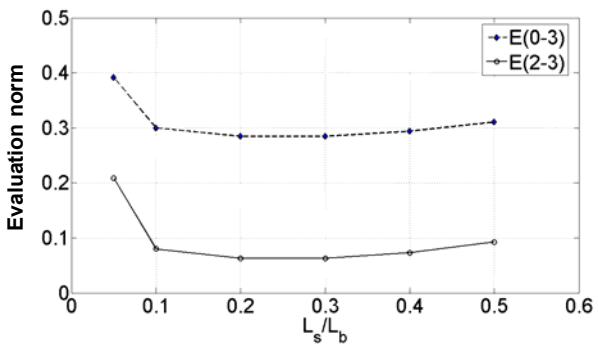

Fig. 5. Norms of normalized tip deflection of cantilever beam for optimum location of piezoelectric actuator

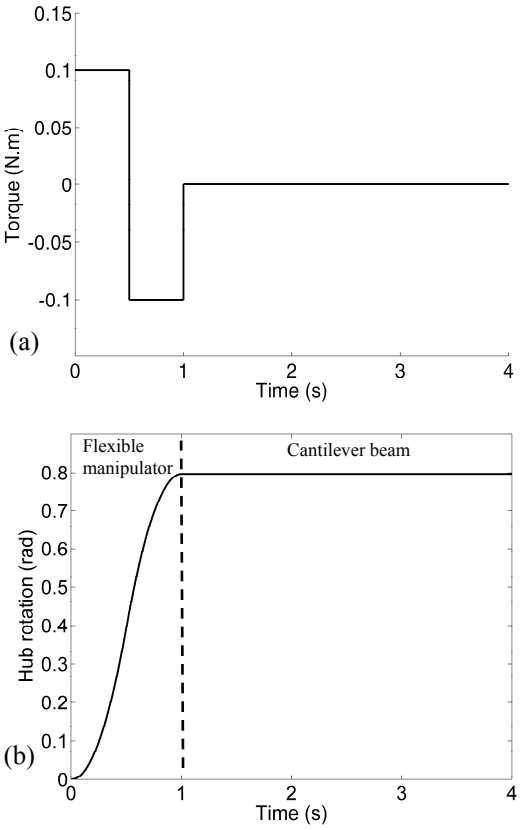

Fig. 6.(a) Applied bang-bang controller torque, and (b) hub rotation.

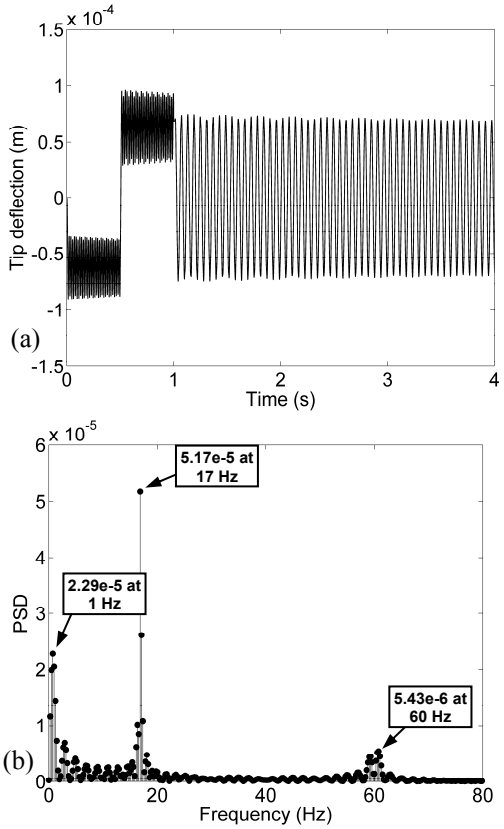

Fig. 7. Case 1 (K_c= 0): Single-link flexible manipulator, (a) tip deflection w.r.t. shadow beam, and (b) FFT spectrum of tip deflection

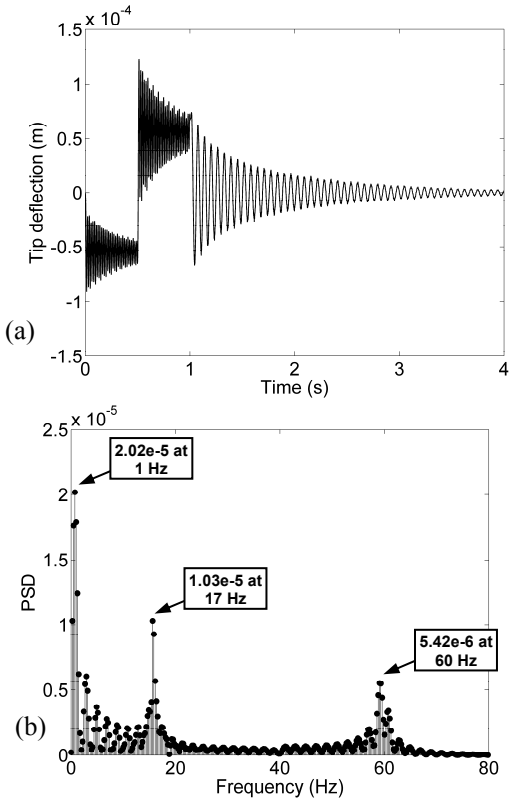

Fig. 8. Case 3 (K_c=4.00e5): Single-link flexible manipulator, (a) tip deflection w.r.t. shadow beam, and (b) FFT spectrum of tip deflection.

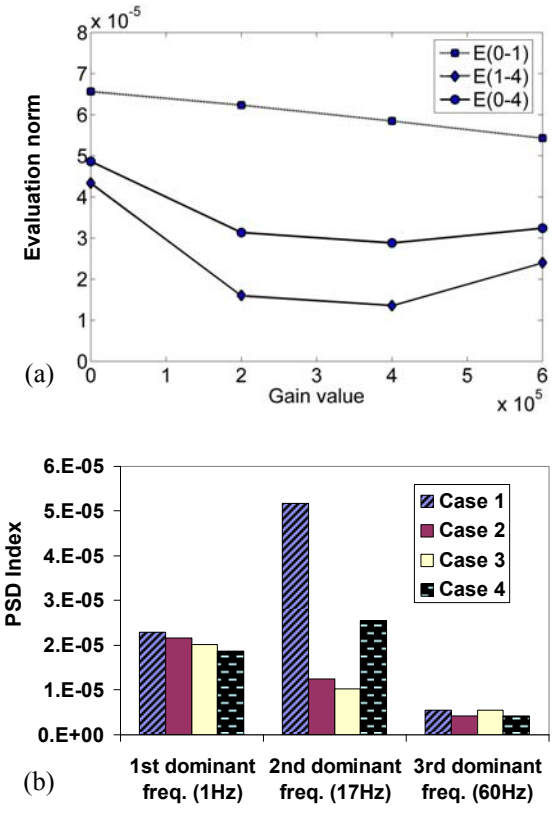

Fig. 9. Single-link flexible manipulator, evaluation criteria for different gain values, (a) norms of vibration amplitudes, and (b) peak values of FFT spectrums at dominant frequencies.